Silver diffusion in commercial QE22 magnesium alloy with Saffil fiber reinforcement

I. Stloukal, J. Čermák

Silver diffusion in commercial QE22 magnesium alloy with Saffil fiber reinforcement

I. Stloukal, J. Čermák

PII: S0266-3538(08)00236-4
DOI: 10.1016/j.compscitech.2008.06.006
Reference: CSTE 4105

To appear in: *Composites Science and Technology*

Received Date: 22 January 2008
Revised Date: 27 May 2008
Accepted Date: 2 June 2008

Please cite this article as: Stloukal, I., Čermák, J., Silver diffusion in commercial QE22 magnesium alloy with Saffil fiber reinforcement, *Composites Science and Technology* (2008), doi: 10.1016/j.compscitech.2008.06.006

Silver diffusion in commercial QE22 magnesium alloy with Saffil fiber reinforcement

I. Stloukal, J. Čermák

Institute of Physics of Materials, AS CR, v. v. i., Žižkova 22, CZ-61662, Brno, Czech Republic

Abstract

Diffusion of ^{110m}Ag in commercial QE22 magnesium alloy with and without short Saffil fibers reinforcement is measured by the radiotracer technique in the temperature interval 648 – 728 K. The obtained diffusion coefficients D_v in the experimental alloys without reinforcement allow to evaluate the influence of the interface between matrix and Saffil fibers on the effective diffusion coefficient D_{eff} and estimate the interface diffusion coefficient D_i of Ag in interphase boundaries. The results obtained for un-reinforced alloy show typical Arrhenius behavior. The pre-exponential factor $D_0 = \left(6^{+5}_{-3}\right)\times10^{-3}\,\mathrm{m^2\,s^{-1}}$ and activation enthalpy Q = 154 ± 3 kJ mol^{-1} are evaluated. It is observed that the temperature dependence of diffusion coefficients D_{eff} and D_i is not Arrhenius-like in the studied temperature interval. This behavior is attributed to relaxation of thermo-elastic stresses in the composite as an effect of large difference between coefficients of thermal expansion (CTE) of Saffil fibers and metal matrix. The maximum values of D_{eff} and D_i, respectively, lies close to 693 K, where CTE has a minimum.

Keywords: A. Metal-matrix composites (MMCs); A. Short-fiber composites; A. Magnesium; B. Interface; B. High-temperature properties; Silver diffusion

1. Introduction

Magnesium-based alloys represent a large group of materials. They are produced in an extent of about 300 000 t/year. They are applied as structural applications, e.g. in military aircraft or automotive industry. They have many excellent physical properties: Mg is the lightest metal, it has high specific strength, good cast ability, etc. [1]. On the other side, there are several properties that limit magnesium for application in industry: low elastic modulus, limited cold workability, limited strength and creep resistance at elevated temperatures, etc. To overcome these unsuitable properties, magnesium is alloyed by other elements and/or some reinforcement is used. Aluminum, zinc, manganese, silver, zirconium and the rare earth metals (RE) are the most frequently used alloying elements; and Al_2O_3 and SiC are used as reinforcing materials.

The commercial creep resistant QE22 alloy is one example of rare earths containing magnesium alloys. Typical compositions of this alloy is Mg-Ag-Di-Zr, where Di is so-called *didymium* – a mixture of RE elements mainly Nd and Pr. Silver alloying improves mechanical properties of magnesium alloys, RE metals increase strength at elevated temperatures and zirconium is very effective grain refiner. Unfortunately, alloying does not improve the elastic properties, such as the Young's modulus. Therefore, the ceramic fibers are suitable to improve stiffness and wear resistance of such metal matrix composites (MMC). The role of the reinforcement on mechanical properties QE22/Al_2O_3/44s MMC including effects on the interface matrix/fibers was intensively studied in recent years, see e.g. in [2-7].

The QE22 alloy is used e.g. as structural material of landing wheels or as rotor heads for helicopters. In these systems, the components are under thermal and

mechanical stress. Therefore, knowledge of diffusion characteristics is very important for evaluation of the rate of such diffusion controlled processes. In the case of MMC, the presence of ceramic fibers creates the matrix/fiber interfaces that may serve as the high diffusivity short-circuit paths. Finally, the considerable difference in the coefficient of the thermal expansion (CTE) of fibers and matrix causes internal stresses during temperature changes and subsequently some stress relaxation phenomena may occur.

The present work deals with measurements of silver diffusion in QE22 magnesium alloy with and without Saffil fiber reinforcement. The experiments were carried out with and without reinforced variant of QE22 alloys in the temperature interval 648–728 K using serial sectioning method. The obtained ^{110m}Ag diffusion coefficients were compared with data on ^{65}Zn diffusion in the same materials in our previous work [8]. The influence of CTE on the temperature dependence of the effective diffusion coefficient D_{eff} and the interface diffusion coefficient D_i will be discussed.

2. Experimental procedure

2.1. Sample preparation

The experimental QE22 magnesium alloy (QE22 is standard ASTM notation [1]) was prepared at the Technische Universität Clausthal-Zellerfeld, Germany by squeeze casting method. The chemical composition of investigated QE22 alloy was Mg – 2.5 wt.% Ag – 2.1 wt.% Di – 0.7 wt.% Zr. The fiber preform consisted of planar randomly distributed Saffil short fibers. The standard composition of them is 97% δ-Al_2O_3 + 3% SiO_2, the mean fiber length is about 50 μm and diameter about 4 μm. The total volume

fraction of Saffil (44 vol.%) was checked by digital image analysis of SEM micrographs.

Samples of QE22 without Saffil fibers (referred to as QE22 hereafter) were machined from marginal part of the ingot, where there was no reinforcement. Core part of the ingot was used for QE22 samples with Saffil fibers (QE22S). The cylinder samples were machined in such a way that the specimen axes were parallel to the plane in which the longitudinal axes of fibers was preferentially situated. The diameter of diffusion specimens was 10 mm and height 4 mm.

The standard T4 heat treatment (798 K / 8 h, water quenching) was used [1]. The samples were wrapped in Ta foils, encapsulated in silica ampoules filled with pure Ar and solution treated as mentioned above in horizontal tube furnace. The temperature was checked by a Pt-PtRh thermocouple with an accuracy of ± 1 K. The subsequent annealing of pre-heated samples was applied to stabilize the structure and grain size of alloys. The respective temperature T and time t were chosen in order to simulate diffusion anneals (Table 1). All temperatures were within the interval, where the only homogenous solid solution of Ag in Mg exists [9].

The final structure of the experimental alloys is show in Figs. 1, 2. The microstructure of QE22 alloy (Fig. 1.) consists of relatively large grains with mean size about 150 μm. The precipitation of Nd-rich phase (bright particles in Fig. 1.) was observed, which is segregated mostly at grain boundaries. Since the QE22 alloy contains more than 2 wt.% Ag, the formation of an equilibrium phase with $Mg_{12}Nd_2Ag$ composition is expected as observed in [10,11]. However, no Ag was detected in those particles by SEM-EDX analysis. Therefore, the presence of such particles can be excluded. All observed precipitates had composition given by a formula $Mg_{9\text{-}12}Di$ and

Ag is solved in the matrix. The same Nd-rich particles were observed in QE22S alloy, but they were preferentially located at the surface of fibers (Fig. 2.), as seen Fig. 3. In the case of QE22S, Saffil fibers might react with the melt during squeeze casting of the samples [12]. However, due to the short melt-fiber contact no interface reactions were observed. Although the precipitation of $(Al_xMg_{1-x})Nd$ phase in similar material was observed by Kiehn et al. [13], no Al content was detected by SEM-EDX analysis in the matrix of the studied QE22S. Therefore, the presence of Al-rich particles can be also excluded in reinforced alloy.

2.2. Radiotracer measurements

The pre-heated samples were metallographically ground and polished using standard methods to achieve a mirror-like quality of the surface. The OP-S suspension (colloidal silica in water, particles mean grain size 0.04 μm) was applied for the last polishing step. The radiotracer ^{110m}Ag was used in the form of an aqueous solution of $^{110m}AgNO_3$ in 1M HNO_3. The specific activity was 57 MBq mg^{-1} of Ag at the beginning of the experiments. The radiotracer was deposited on the sample surface using the vacuum evaporation technique in the following way: first, the carrier was dripped-and-dried onto a tungsten boat, then it was thermally decomposed in vacuum (~ 3×10^{-6} mbar) and finally, it was evaporated onto cold samples. After that, the samples was wrapped in Ta foil, encapsulated in silica ampoules filled with pure Ar and annealed at selected temperatures T and diffusion times t (Table 1) in a horizontal furnace stabilized within ± 1 K.

After diffusion treatment, the cylindrical samples were reduced in diameter to eliminate any possible effects of surface diffusion. The penetration profiles were obtained by the serial sectioning method along the samples' faces. The thin layers of about 2 – 5 μm were removed from the sample surface by the Fully Motorized Rotary Microtome Leica RM2255. Each layer was carefully placed into a plastic vial and solved with 0.6 cm^3 of HCl solution (2 cm^3 conc. HCl + 100 cm^3 distilled water). After dissolution of the layers, each vial was filled with scintillation cocktails Ultima Gold.

The isotope ^{110m}Ag has a half-life 249.85 days and decays by emission of electrons with a maximum energy level 529 keV into stable isotope ^{110}Ag. The activity of each dissolved layer $c(x,t)$, where x is penetration depth, was measured with a great efficiency using Liquid Scintillation Counter TRI-CARB 3170 TR/LS equipped with an automatic sample changer.

3. Results and discussion

3.1. Penetration profiles

The measured penetration profiles are shown in Figs. 4, 5 in co-ordinates log c vs. x^2. As can be seen, there is good linearity of profiles over about 2 decades. This fact gives possibility to describe diffusion by volume diffusion coefficient D_v in non-reinforced QE22 alloy and by effective diffusion coefficient D_{eff} in reinforced one [14]. The diffusion coefficients D_v and D_{eff} were obtained by fitting thin-source solution [15]

$$c(x,t) = \frac{M}{\sqrt{\pi D t}} \exp\left(-\frac{x^2}{4Dt}\right), \quad (1)$$

where M stands for surface concentration of diffusant at $t = 0$, D is either volume diffusion coefficient D_v or effective diffusion coefficient D_{eff}. Eq. (1) was fitted to measured penetration profiles and constants D and M were found as fit parameters. The obtained diffusion coefficients D are listed in Table 1. Typical relative error was about 5% by D_v and 20% by D_{eff}. The near-surface part of the penetration profiles was excluded from the fitting procedure because of imperfection of first several cuts.

The values of mean diffusion path in the bulk, L, are listed in Table 1. With respect to microstructure of QE22S alloy in Fig. 2., it is clear that values of L are much greater than the typical distance between the fibers, and, at the same time, much greater than the typical diameter of fibers. Hence, it can be concluded that the diffusion in the reinforced alloy can be well described by an effective diffusion coefficient D_{eff} [14].

3.2. Effective diffusivity

As can be seen in Table 1, the values of D_{eff} are greater than those of D_v, except at 728 K. If we suppose that volume diffusion in alumina in general is much slower [16] than in QE22, it may be concluded that the difference between D_{eff} and D_v is due to the fast diffusion along interface Saffil/matrix. Belova and Murch [17] have proposed the following relation between the effective diffusivity D_{eff} in two phases and interphase boundary diffusivity D_i

$$D_{eff} = \left(\frac{D_i}{g_i + \frac{g_1}{s_1} + \frac{g_2}{s_2}} \right) \frac{1 - 2g_1 \frac{D_i s_1 - D_1}{2D_i s_1 + D_1} - 2g_2 \frac{D_i s_2 - D_2}{2D_i s_2 + D_2}}{1 + g_1 \frac{D_i s_1 - D_1}{2D_i s_1 + D_1} + g_2 \frac{D_i s_2 - D_2}{2D_i s_2 + D_2}}. \quad (2)$$

The indices 1 and 2 denote the individual phases; g and s are volume fractions and segregation factors of respective phases. If we assume in the present case that silver diffusivity in the interfaces is much faster than that in alumina and in the matrix, i.e. $D_i >> D_1, D_2$, and that silver does not segregate too much to the near-surface area both in the matrix and fibers, i.e. s_1, s_2 ~ 1, the Eq. 2 can be simplified to

$$D_i = \frac{2 + g_1 + g_2}{2 g_i} D_{eff} . \quad (3)$$

Then, for the known volume fraction of fibers g_1 ~ 0.44 in QE22S, g_i can be estimated using the following values: typical diameter of fibers was about 4 μm and length 50 μm, and thickness of interface $\delta \sim 5 \times 10^{-10}$ m (commonly accepted grain boundary thickness [14]). Thus the final relation can be written as

$$D_i \cong 7 \times 10^3 D_{eff} . \quad (4)$$

Calculated values of D_i are summarized in Table 1. Their typical relative error was about 63%.

3.3. Temperature dependence of D_v

The temperature dependence of the obtained volume diffusion coefficients D_v in QE22 alloy are shown in Fig. 6. It can bee seen that the experimental points can be described by the Arrhenius relation - straight line fitted to full points in Fig. 6. The diffusion characteristic, i.e. pre-exponential factor D_0 and activation enthalpy Q, are listed in Table 2 together with literature data.

As it can be seen in Fig. 6, the obtained diffusion coefficients of Ag in QE22 alloy are lower than those for Zn diffusion in the same material [8]. This result can be

explained by the relation between atomic radii of elements [20] (r_{Ag} = 0.16 nm and r_{Zn} = 0.135 nm, respectively) – the greater radius, the slower diffusivity of respective elements. The similar ratio of known diffusivity of the same elements can be seen for polycrystalline Mg (see Table 2). However in this case, the effect of atomic radii is not so expressive as for Ag and Zn diffusion in QE22 alloy.

3.4. Temperature dependence of D_{eff} and D_i

In comparison with D_v, the temperature dependences of Ag diffusion coefficients D_{eff} and D_i show obviously a non-Arrhenius behavior in the measured temperature interval 648 – 728 K. The deviation from the standard Arrhenius behavior is illustrated in Fig. 6 by dashed lines (they guide the eye only). The values of both diffusion coefficients D_{eff} and D_i, respectively, have a tendency to higher values in the middle of measured temperature interval. This behavior supports our previous observations dealing with zinc diffusion in QE22S alloy [8].

The explanation of such an effect can be explained using the temperature dependence of local strain close to the matrix/fiber interfaces. Rudajevová and Padalka [5] have studied thermal expansion of magnesium composites reinforced by Saffil fibers. It was observed that above the certain inverse temperature T_i, the CTE of composite starts to decrease with increasing of temperature and it goes through a local minimum $T_{CTE\ min}$.

There are three concurrent processes running parallel. (i) The volume diffusion described by coefficient D_v, which increases with increasing temperature due to the thermal activation. This process is described by the Arrhenius equation. (ii) Increasing

strain localized by interphase plane (matrix/fiber), which also increases with increasing temperature due to considerably different CTE. This leads, after the limits of elastic accommodation is exhausted, to an increase of dislocation density. (iii) With increasing the temperature, the recovery of dislocations also proceeds. This is more pronounced at higher temperatures.

Therefore, it can be supposed that all these effects superimpose one over another resulting in the increasing dislocation density up to the temperature about 688 K and decreasing dislocation density at higher temperatures. This leads to the observed break on the temperature dependence of D_{eff} a D_i as can be seen in Fig. 6.

4. Conclusions

The investigation of ^{110}Ag diffusion in magnesium-based QE22 alloy with and without Saffil fiber reinforcement yield the following conclusions:

1. The diffusion experiments were carried out in the temperature interval 648 – 728 K. The obtained penetration profiles were used to calculate volume diffusion coefficients D_v in the case of QE22 alloy and effective diffusion coefficients D_{eff} in the case of QE22S alloy.
2. The observed relation $D_{eff} > D_v$ invokes that the effective diffusivity in QE22S alloy consists of two contributions: the volume diffusion and the fast diffusion along the interface short Saffil fibers/matrix.
3. The interphase boundary diffusivity D_i was estimated using the theoretical relation between D_{eff} and D_i, known geometrical properties of the Saffil fibers

and the commonly used value of width of the interface boundary. The relation between D_{eff} and D_i can be written as $D_i \cong 7\times10^3 D_{eff}$.

4. The temperature dependence of volume diffusion has Arrhenius behavior. The relevant parameters are $D_0 = 6 \times 10^{-3}$ m^2 s^{-1} and Q = 154 kJ mol^{-1}. The silver volume diffusion coefficients are lower than analogous values of ^{65}Zn diffusion reported in our previous work [8].
5. Similar to ^{65}Zn diffusion coefficients, the up-ward curvature of ^{110m}Ag coefficients D_{eff} and D_i was observed close to $T_{CTE\ min}$. This observation is probably caused by increasing dislocation density up to T ~ 688 K and its decrease at higher T as result of recovery.

Acknowledgements

The work was supported by the Czech Science Foundation (project No. 106/05/2115) and by the Academy of the Sciences of the Czech Republic (project No. AV0Z20410507).

References

[1] Avedesian M, Baker H. Magnesium and Magnesium Alloys. ASM Materials Park; 1999.

[2] Lukáč P, Rudajevová A. Thermal expansion in magnesium composites. Kovove Mater 2003;41:281–292.

[3] Rudajevová A, Balík J, Lukáč P. Thermal expansion behaviour of Mg-Saffil fibre composites. Mater Sci Eng A 2004;387–389:892–895.

[4] Kumar S, Mondal AK, Dieringa H, Kainer KU. Analysing hysteresis and residual strains in thermal cycling curves of short fibre reinforced Mg-MMCs. Compos Sci Technol 2004;64:1179–1189.

[5] Rudajevová A, Padalka O. Thermal expansion of pre-deformed, short fibre reinforced Mg-based composites. Compos Sci Technol 2005;65:989–995.

[6] Rudajevová A, Musil O. Influence of the interface on the thermal expansion and thermal conductivity of QE22 based composites. Kovove Mater 2005;43:210–217.

[7] Mielczarek A, Trojanová Z, Riehemann W, Lukáč P. Influence of mechanical cycling on damping behaviour of short fibre-reinforced magnesium alloy QE22. Mat Sci Eng A 2006;442:484–7.

[8] Čermák J, Stloukal I. Diffusion of ^{65}Zn in AZ91 and in QE22 reinforced by Saffil fibers. Compos Sci Tech 2008;68,417-23.

[9] Massalski TB. Binary alloy phase diagram. ASM International, ASM/NIST, CD-ROM; 1996.

[10] Polmear IJ. Magnesium alloys and applications. Mater Sci Technol 1994;10:1-16.

[11] Rakowska A, Socjuzs-Podosek M, Litynska L, Ciach R. Analytical electron microscopy of magnesium alloy containing neodymium. Microchim Acta 2002;139:145-9.

[12] Rehman FU, Fox S, Flower HM, West DRF. Fibre/matrix interactions in magnesium-based composites containing alumina fibres. J Mater Sci 1994;29:1636-44.

[13] Kiehn J, Smola B, Vostrý P, Stulíková I, Kainer KU. Microstructure changes in isochronally annealed alumina fibre reinforced Mg-Ag-Nd-Zr alloy. Phys Status Solidi (a) 1997;164:709–23.

[14] Kaur I, Mishin Y, Gust W. Fundamentals of grain and interphase boundary diffusion. Chicester, New York, Brisbane, Toronto, Singapore: J. Wiley & Sons; 1995.

[15] Crank J. Mathematics of diffusion, Oxford: Clarendon Press; 1957.

[16] Le Gall M, Lessage B. Self-diffusion in α-Al_2O_3 I. Aluminium diffusion in single crystals. Philos Mag A 1997;70:761–63.

[17] Belova IV, Murch GE. The effective diffusivity in polycrystalline material in the presence of interphase boundaries. Philos Mag 2004;84:17–28.

[18] Combronde J, Brebec G. Heterodiffusion de Ag, Cd, In, Sn et Sb dans le magnesium. Acta Metall 1972;20:37–44.

[19] Lal K. CEA Report 1967;R3136:54.

[20] Slater CJ. Atomic radii in crystals. J Chem Phys 1964;39:3199-204.

Table 1

Volume diffusion coefficients D_v in QE22 alloy, effective diffusion coefficients D_{eff} and diffusions coefficients D_i in interfaces between the matrix and Saffil fibers in QE22S alloy.

T [K]	t [s]	D_v [m^2 s^{-1}]	$L = 2\sqrt{D_v t}$ [μm]	D_{eff} [m^2 s^{-1}]	D_i [m^2 s^{-1}]
728	7200	6×10^{-14}	40	3×10^{-14}	2×10^{-10}
708	18000	3×10^{-14}	46	6×10^{-14}	4×10^{-10}
688	25200	1×10^{-14}	36	6×10^{-14}	4×10^{-10}
668	54000	6×10^{-15}	37	2×10^{-14}	2×10^{-10}
648	72000	2×10^{-15}	27	5×10^{-15}	3×10^{-11}

Table 2

Arrhenius parameters for ^{110}Ag diffusion in QE22 alloy in comparison with ^{110}Ag solute diffusion in pure Mg single crystal and with ^{65}Zn diffusion in QE22 alloy.

Material	Diffusant	D_0 [m^2 s^{-1}]	Q [kJ mol^{-1}]	Reference
QE22	^{110m}Ag	$\left(6^{+5}_{-3}\right)\times10^{-3}$	154 ± 3	this work
QE22	^{65}Zn	9×10^{-5}	125	[8]
single crystal Mg (∥ to *c*-axis)	^{110m}Ag	4×10^{-4}	133	[18]
single crystal Mg (⊥to *c*-axis)	^{110m}Ag	2×10^{-3}	148	[18]
polycrystalline Mg	^{65}Zn	4×10^{-5}	120	[19]
polycrystalline Mg	^{110m}Ag	3×10^{-5}	119	[19]

Figure captions

Fig. 1. SEM micrograph of QE22 after T4 + 728 K / 2h treatments. Polished with diamond paste; secondary electron image (SEI). Bright Nd-rich precipitates.

Fig. 2. SEM micrograph of QE22S after T4 + 728 K / 2h treatments. Polished with OP-S suspension; secondary electron image (SEI).

Fig. 3. SEM micrograph of QE22S after T4 + 728 K / 2h treatments. Polished with OP-S suspension; secondary electron image (SEI). Small bright Nd-rich precipitates mostly decorate the fiber/matrix interfaces.

Fig. 4. Penetration profiles for ^{110m}Ag diffusion in QE22 alloy measured after variations of the annealing period at different temperatures (Table 1).

Fig. 5. Penetration profiles for ^{110m}Ag diffusion in QE22S alloy measured after variations of the annealing period at different temperatures (Table 1).

Fig. 6. Arrhenius plot of measured ^{110m}Ag diffusion coefficients in QE22 and in the fiber reinforced alloy – full symbols compared with data on ^{65}Zn diffusion in the same material [8] – empty symbols.

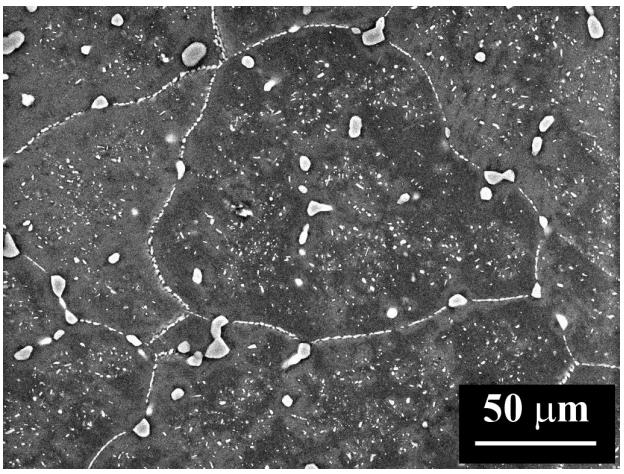

Fig. 1.

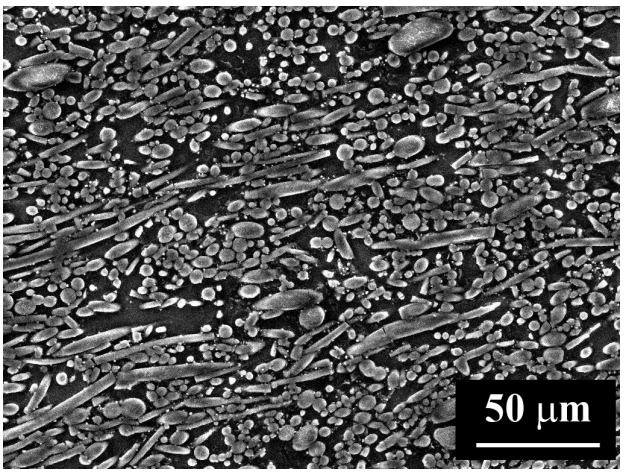

Fig. 2.

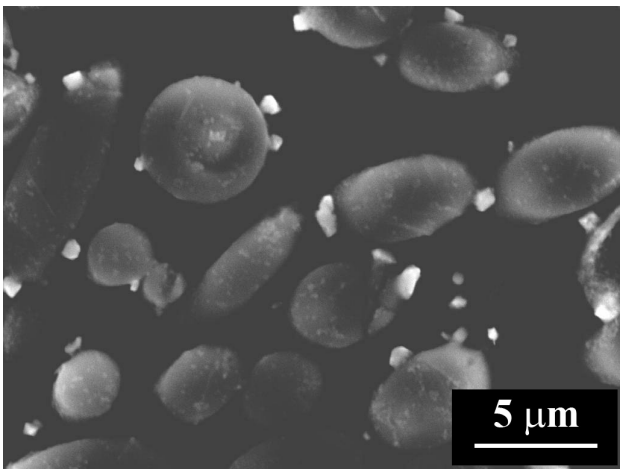

Fig. 3.

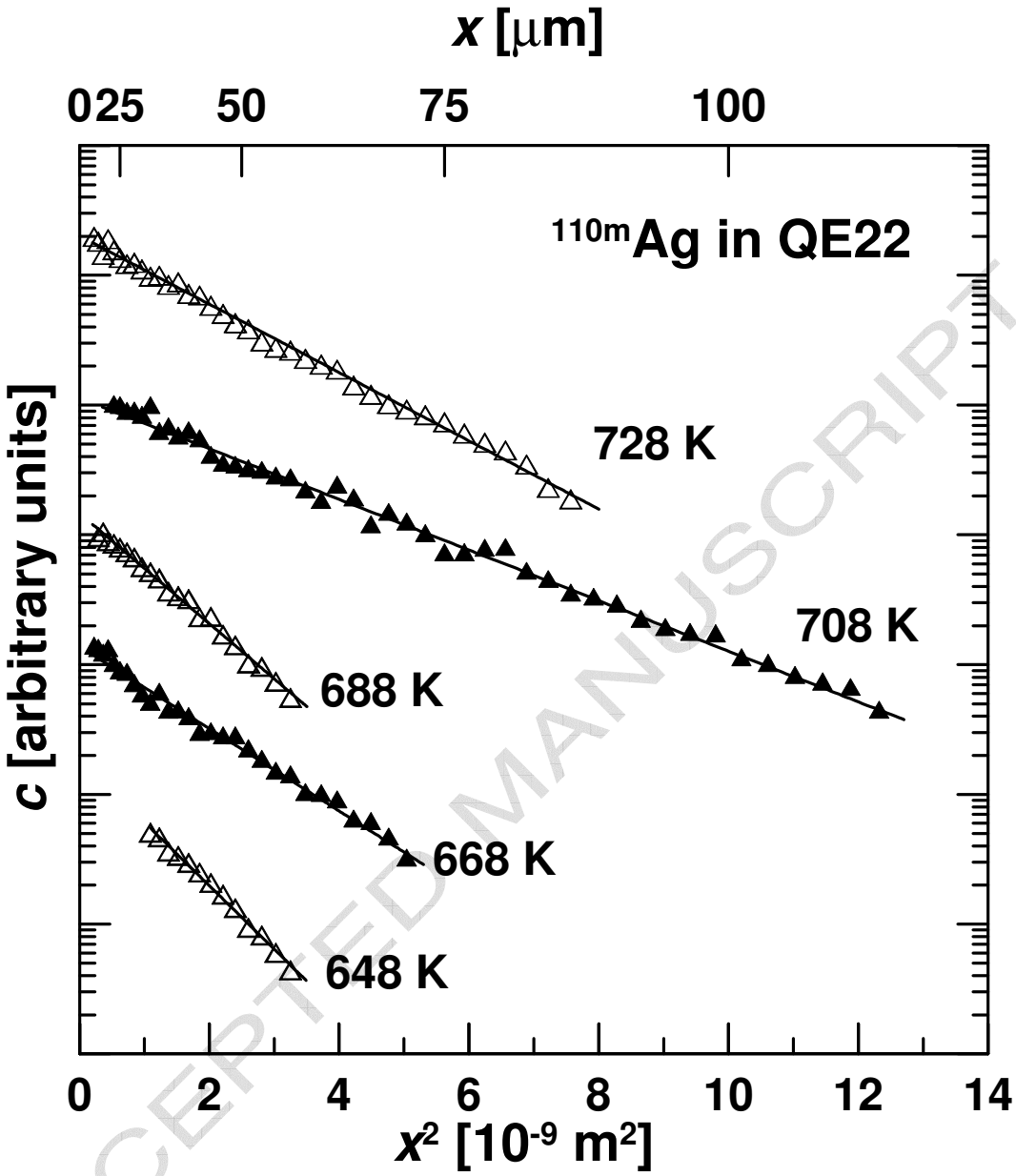

Fig. 4.

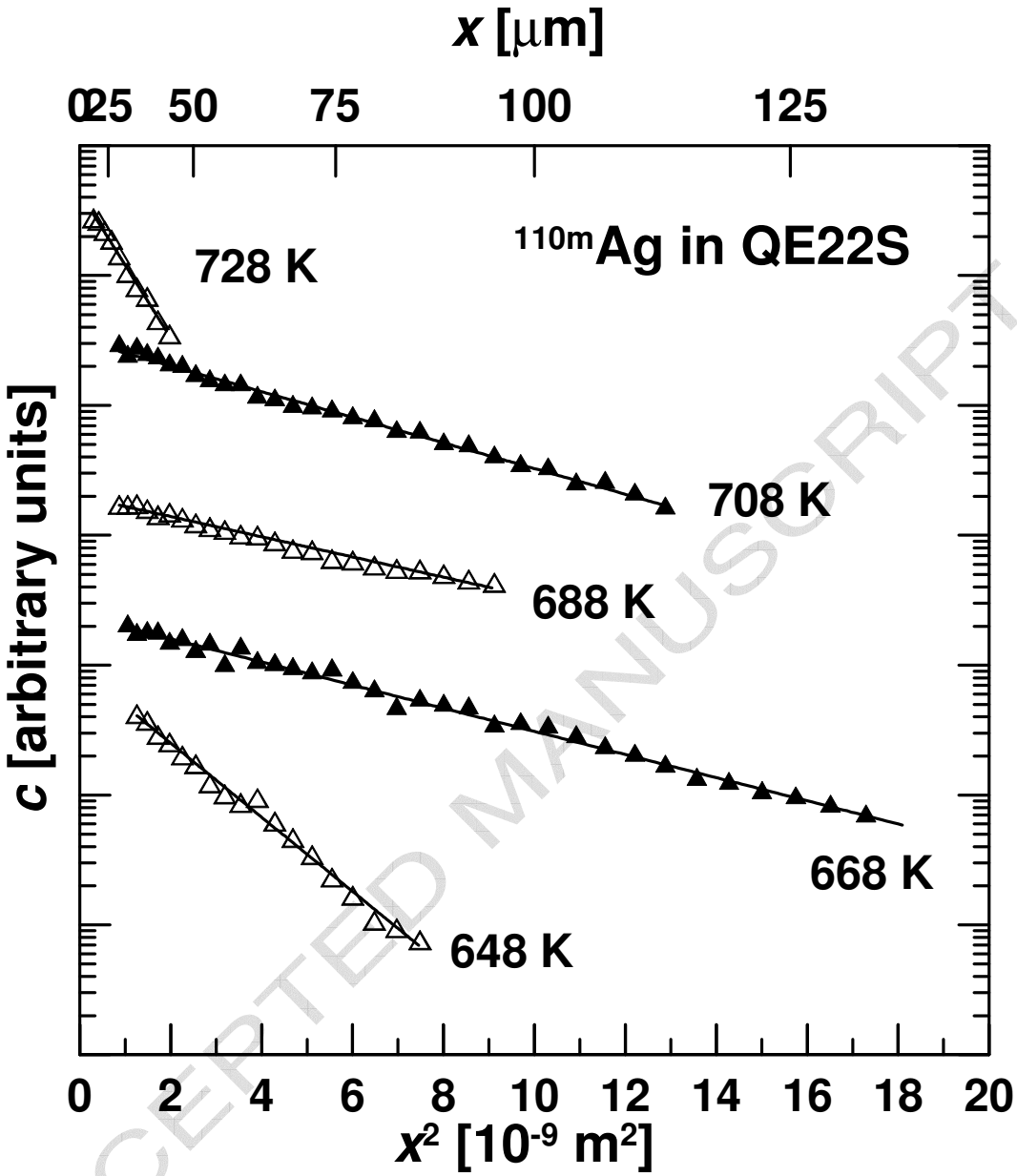

Fig. 5.

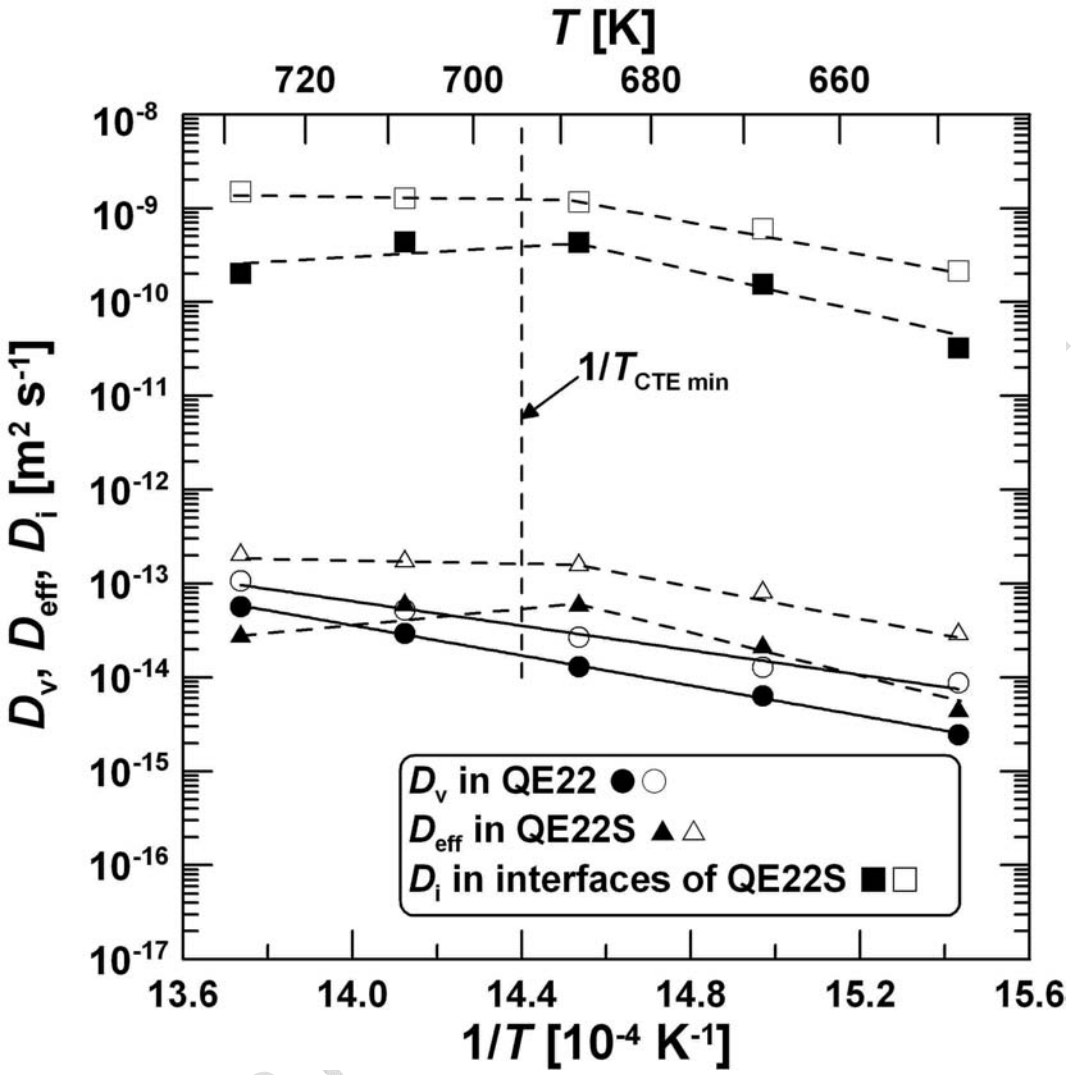
T [K]
720
700
680
660
10-8
10-9
10-10
10-11
10-12
10-13
10-14
10-15
10-16
10-17
Dv, Deff, Di [m2 s-1]
1/TCTE min
Dv in QE22 ●○
Deff in QE22S ▲△
Di in interfaces of QE22S ■□
13.6
14.0
14.4
14.8
15.2
15.6
1/T [10-4 K-1]

Fig. 6.